Typical meteorological conditions associated with extreme nitrogen dioxide (NO_2) pollution events over Scandinavia

Manu Anna Thomas and Abhay Devasthale

Research and development department, Swedish Meteorological and Hydrological Institute (SMHI), Folkborgsvägen 17, 60176 Norrköping, Sweden

Correspondence: manu.thomas@smhi.se

Abstract

Characterizing typical meteorological conditions associated with extreme pollution events helps in the better understanding of the role of local meteorology in governing the transport and distribution of pollutants in the atmosphere. The knowledge of their co-variability could further help to evaluate and constrain chemistry transport models (CTMs). Hence, in this study, we investigate the statistical linkages between extreme nitrogen dioxide (NO_2) pollution events and meteorology over Scandinavia using observational and reanalysis data. It is observed that the south-westerly winds dominated during extreme events, accounting for 50-65% of the total events depending on the season, while the second largest annual occurrence was from south-easterly winds, accounting for 17% of total events. The specific humidity anomalies showed an influx of warmer and moisture-laden air masses over Scandinavia in the free troposphere. Two distinct modes in the persistency of circulation patterns are observed. The first mode lasts for 1-2 days, dominated by south-easterly winds that prevailed during 78% of total extreme events in that mode, while the second mode lasted for 3-5 days, dominated by south-westerly winds that prevailed during 86% of the events. The combined analysis of circulation patterns, their persistency, and associated changes in humidity and clouds suggests that NO_2 extreme events over Scandinavia occur mainly due to the long-range transport from the southern latitudes.

1. Introduction

Nitrogen dioxide (NO_2) is one of the highly reactive gases of the nitrogen oxides (NOx) family. The major sources of NO_2 are fuel combustion in motor vehicles, industrial boilers, emissions from soil and agricultural biomass burning. The natural source of NO_2 is lightning and forest fires. Recent studies indicate increasing trends in NO_2 in developing countries and decreasing trends in developed countries as a result of environmental regulation policies (Richter et al. 2005; Zhang et al. 2007; van der A et al. 2008; Schneider et al. 2015; Geddes et al. 2016). NO_2 is an oxidizing agent resulting in the corrosive nitric acid and plays an important role aiding the formation of ozone. It can also contribute to the formation of particulate matter (PM) and secondary organic particles through photochemical reactions. Increased NOx concentrations not only severely affect human physical health through reduced lung function, but also affect aquatic ecosystems through acid deposition and eutrophication of soil and water (Sjöberg et al. 2004; Klingberg et al. 2009; Bellandar et al. 2012; Gustafsson et al. 2014; Nilsson Sommar et al. 2014; Oudin et al. 2016; Taj et al. 2016). Lamarque et al. (2013) based on the multi-model intercomparison assessed increases in regional nitrogen deposition by up to 30-50% from RCP 2.6 to RCP 8.5. According to the 4th IPCC Assessment Report, the total global NOx emissions have increased from a pre-industrial value of 12 Tg N/yr to between 42 and 47 Tg N/yr in 2000. The most recent study by Miyazaki et al. (2017) estimated a ten year (2005-2014) global total surface NOx emissions of 48.4 Tg N/year with an increase of 29%, 26% and 20% per decade increase respectively over India, China and Middle East and a decrease of 38%, 8.2% and 8.8% respectively over United States, southern Africa and western Europe. In heavily polluted areas NO_2 can also have noticeable impact on the local radiation budget (Vasilkov et al. 2009).

Compared to other pollutants such as carbon monoxide (CO) that has a life span of weeks to few months, NO_2 has a relatively shorter life time in the atmosphere and ranges typically from a couple of hours in the boundary layer to up to few days in the upper troposphere (Beirle et al., 2011). Therefore, NO_2 can be typically associated with short-range transport events. For long range transport (LRT) or intercontinental transport of pollutants and in particular of NO_2 to occur, the associated weather systems need to be linked with stronger winds and rapid convective-advective events such as cyclones or warm conveyor belts (WCBs) that can lift air masses from their source regions up into the free troposphere and be transported across the oceans (Eckhardt et al. 2003; Stohl et al. 2003). Due to lower concentrations of radical species in the free troposphere, the reaction with NO_2 is limited. Zien et al. (2014) identified about 3800 LRT events of NO_2 during a 5 year period from the major pollution hotspots such as the east coast of North America, central Europe, China and South America, predominantly during autumn and winter months.

There have been several studies reporting individual LRT events of NO_2. To mention a few, Stohl et al. (2003) in a study explained “intercontinental express highways” being responsible for almost 60% of the total intercontinental transport of pollutants from across the Atlantic to Europe, resulting in an increment of average European winter NOx mixing ratios by about 2-3 pptv. In yet another study, Schaub et al. (2005) demonstrated that at least 50 % of the NO_2 recorded at the Alpine region was advected via a frontal system from the Ruhr area in central Germany in February 2001. Donnelly et al. (2015) reported that easterly air masses during winter resulted in increased NO_2 concentrations in the urban and rural sites in Ireland. LRT of NOx across the Indian Ocean from South Africa to Australia in May 1998 was reported by Wenig et al. (2003).

The Nordic countries often lie at the receiving end of short-range pollutant transport from northern Europe or they are a part of a much larger transit pathway of eventual long-range transport to the Arctic, originating from either Europe or North America. To what extent such a transport from the southerly latitudes affects the characteristics of extreme pollution events (such as magnitude, frequency and persistence) over Scandinavia depends largely on prevailing circulation patterns and meteorological conditions. The local meteorology can enhance or dampen the concentration of the pollutants depending on the degree of persistency; the knowledge of which would help to better constrain the chemistry transport models (CTMs). Therefore, identifying the dominant weather patterns over Scandinavia especially during extreme pollution is important. However, there has not been a systematic study linking the transport events of NO_2 to different meteorological conditions, solely from observational data over the Scandinavian region. Therefore, the main aim of the present study is to characterize circulation regimes and meteorological conditions extreme pollution events, to understand to what extent they differ from climatological conditions. There are two different ways to study this co-variability solely using observational data: 1) the “top- down approach” wherein the atmospheric state is first identified and then the variability of the tracers is evaluated. This approach gives a general perspective of the distribution of tracers based on a particular weather state and 2) the “bottom-up approach” wherein the pollution episode is first identified and the weather state associated with it is studied. In this study we make use of the bottom-up approach as explained in the next section.

2. Data sets and methodology

The NO_2 tropospheric column densities from OMI (Ozone Monitoring Instrument) on board the EOS Aura satellite are used in this study to define and identify extreme events (Boersma et al., 2001, 2008, 2011; Bucsela et al., 2006, 2008, 2013; Lamsal et al. 2008, 2010, 2014). 11 years (2004 – 2015) of daily Level 3 gridded standard product, available at 0.25x0.25 degrees resolution is analysed (OMNO2d, Version 3, available at: https://disc.gsfc.nasa.gov/Aura/data-holdings/OMI/omno2d_v003.shtml). This particular product is used as it provides good quality OMI retrievals, already screened based on recommendations by the OMI Algorithm Team. We allowed retrievals under cloudy conditions to be analysed, not only to have robust number of samples, but also to avoid clear-sky biases since the NO_2 transport is often associated with cyclonic systems that lead to increased cloudiness (Zien et al. 2014). We further tested the sensitivity of our results to using only cloud screened retrievals, to evaluate if the selection of extreme events and associated meteorological conditions are different from those cases when retrievals under partially cloudy conditions are used.

Humidity and cloud fraction retrievals from the AIRS (Atmospheric Infrared sounder) instrument on board Aqua satellite are used (Chahine et al. 2006; Susskind et al. 2014; Devasthale et al. 2016). Both Aqua and Aura satellites are a part of NASA's A-Train convoy, providing added advantage of simultaneous observations of trace gases from OMI-Aura and thermodynamical information from AIRS-Aqua. AIRS Version 6 Standard Level 3 Daily Product (AIRX3STD) for the same period (2004-2015) is used (data available at: https://disc.gsfc.nasa.gov/uui/datasets?keywords=%22AIRS%22).

To investigate circulation patterns, u and v wind components at 850 hPa from ECMWF's ERA-Interim Reanalysis are used (Dee et al., 2011; http://apps.ecmwf.int/datasets/data/interim-full-daily/levtype=sfc/).

In order to investigate co-variability of meteorological conditions and pollutants using observations, two different approaches can be taken (Fig. 1). In a "top-down" approach, a weather state classification can be done to identify most prevailing weather states that occur over the study area and then the relative distribution of pollutants can be investigated under those states to rank them. This approach was adapted by Thomas and Devasthale (2014) and Devasthale and Thomas (2012). In a "bottom-up" approach on the other hand, a set of pollution events can be identified first and then the corresponding meteorological conditions can be investigated. This bottom-up approach is the focus of the present study. It should be mentioned that both of these approaches have their advantages and limitations. For example, the dominant weather pattern identified in the top-down approach may not have the largest impact on pollutant variability and the pollution events identified in the bottom-up approach may not be associated with the dominant weather pattern or may not have the largest impact on an average in the weather state they occur. Therefore, only the combination of these two approaches will provide a complete picture of the co-variability between meteorological conditions and pollutants.

In the present study, an “extreme” pollution event is defined as follows. First, the histograms of NO_2 tropospheric column densities using OMI data for each month are computed over the centre of the study area (55N-60N, 11E-20E). This area is chosen because it accommodates top ten polluted and populated cities/regions in Sweden (Sjöberg et al. 2004; Klingberg et al. 2009; Bellandar et al. 2012; Gustafsson et al. 2014; Nilsson Sommar et al. 2014; Oudin et al. 2016; Taj et al. 2016). All events that surpass the 90-percentile (90%ile) value are considered as extreme events. The monthly histograms of NO_2 over the study region are shown in Fig. 2 along with 90 percentile thresholds for each month (vertical lines). Since NO_2 distributions over the study area show strong monthly variability, the monthly thresholds were chosen to define extreme events. The distributions of NO_2 have longer tails during winter half year and the tropospheric columns are also higher. Therefore, the resulting 90%ile thresholds are also higher in winter compared to summer months. However, using thresholds based on percentiles (rather than having a fixed value throughout the season or year), makes the criteria for the selection of extreme events fair and equally applicable for each month.

3. Meteorological conditions observed during extreme events

The spatial distribution of tropospheric NO_2 column during climatological conditions, extreme events and anomalies thereof is presented in Fig. 3. Note that although the thresholds for defining extreme events are different for each month, the results are compiled over four distinct seasons for the sake of brevity. By definition, NO_2 anomalies during extreme events are similar in magnitude to climatological values over Scandinavia. The spatial extent of the severity of the extreme pollutant episodes over southern Sweden is noticeable. Under climatological conditions, highest concentrations are observed over northern Germany and France, the Netherlands and Belgium (the Benelux region). There is a good spatial coherence between NO_2 distributions under climatological conditions and extreme events, in the sense that the high concentrations of NO_2 seemed to have spread over southern Scandinavia during extreme events from the regions where climatological values are usually higher. It is to be noted that during extreme events the pollution levels over northern European regions are also enhanced. For an event to qualify as an extreme event over southern Scandinavia, the pollutant levels in the source regions also need to be higher than usual in order to allow strong transport under favourable atmospheric circulation patterns. This provides confidence in the selection process of extreme events. The NO_2 concentrations are relatively higher in winter and autumn compared to the summer months. This is mainly because atmospheric removal by radical species and deposition are much more efficient in the summer months.

In order to characterize typical meteorological conditions that can result in such high concentrations over Scandinavia, we first investigated the dominant wind direction at 850 hPa associated with those extreme events using ERA-Interim reanalysis data. The normalized frequency of occurrence of different wind directions during four seasons is shown in Fig. 4. It can be seen that, irrespective of the season, the south-westerly winds are dominant during extreme events accounting for 50-65% of total events. This is consistent with south-westerly extension of pollution plume mentioned earlier. The second largest annual occurrence is from south-easterly winds, accounting for 17% of total events followed equally similar contribution from north-westerly winds. Compared to climatological conditions, south-westerly winds have 30-40% more likelihood of being dominant during extreme events depending on the season. However, such clear tendency compared to climatological conditions is not observed in the case of other wind directions. The spatial pattern of the 850 hPa winds based on ERA-Interim reanalysis and corresponding humidity anomalies at 850 hPa based on AIRS data during extreme events are shown in Figs. 5 and 6 respectively. A clear transport pathway from the northern continental Europe to Scandinavia is visible. The strongest winds are observed during the DJF months followed by the SON months with average wind speeds reaching over 10 m/s. The weakest winds are observed during the JJA months. The circulation pattern is characterized by the presence of low pressure systems in the Norwegian Sea that create favourable conditions for the transport of pollutants from continental Europe into Scandinavia. The location of the center of these cyclonic systems can slightly vary over the Norwegian Sea, affecting the direction and strength of the northward flow, as evident in Fig. 5. For example, in the DJF months, the center is located far away in the open Norwegian Sea allowing stronger south-westerly winds over southern Scandinavia. In the JJA months, the center of cyclonic systems is close to western Norwegian coast. While this pattern also leads to south-westerly winds, air masses are mixed with colder and drier air from the northern Norwegian Sea.

The specific humidity anomalies show an influx of warmer and moister air masses over Scandinavia (Fig. 6), except in summer as mentioned above. The seasonality in the vertical structure of the specific humidity anomalies over Scandinavia is shown in Fig. 7c. While there are large deviations in humidity anomalies, influenced by the strength of the wind flow, they are positive regardless of the season during extreme events and peak at 2-3 km above the surface. Such increase in the free tropospheric moisture, especially during winter half year in the absence of local moisture sources, can only be explained by the transport from southern latitudes. The vertical water vapour anomalies are higher in winter half year (DJF and SON), consistent with high NO_2 anomalies during those months. Fig. 8 further shows cloud fraction anomalies. Average cloudiness is increased in all seasons during extreme events, in particular during winter half year. During this time of year, the large-scale frontal systems originating from the southwesterly regions can bring moister airmasses over Scandinavia, as can be seen in the circulation patterns and humidity anomalies, creating favourable conditions for cloud formation. Therefore, these positive cloud fraction anomalies, in combination with positive humidity anomalies and circulation patterns, are indicative of the long-range transport of airmasses associated with increased NO_2 concentrations.

For an extreme pollution event to be linked with the transport the wind flow should be stronger allowing rapid advection and associated circulation pattern also needs to be persistent. Fig. 7a and 7b show the histograms of wind speed at 850 hPa over the study areas during extreme events when data are partitioned by wind direction and by season respectively. The average values of wind speeds are also shown for extreme events and climatological conditions (in brackets). Although the distributions are shifted to higher wind speeds in nearly all cases during extreme events compared to climatological conditions, the average wind speeds are not significantly different. The south-westerly winds are strongest and show largest difference in average wind speeds, while the northeasterly winds are weakest. Average wind speeds during the winter half year (DJF and SON) are higher than the summer half year, consistent with observed positive anomalies of humidity and clouds.

The persistency of the different circulation patterns during these extreme events is further evaluated as shown in Fig. 7d. The persistency is defined as follows. If an extreme event is observed, the wind speed and wind direction are computed for the last 10 days. It is then checked how many days back in time that particular wind direction was *continuously* sustained and that wind direction is not changed by more than $\pm 15^0$ (a third of the quadrant) during that time period. It is to be noted that the choice of the $\pm 15^0$ threshold is based on the visual inspection of about 25 test cases. It was found that if a stricter threshold is used (requiring wind direction deviations less than $\pm 5^0$) the sampling is considerably reduced for long persistency events. On the other hand, if a more relax threshold is used (allowing deviations up to $\pm 30^0$) we incorporate tail ends of the events that persisted over neighbouring areas. Two distinct modes in the persistency of circulation patterns are observed, one in which a particular wind direction persists for a day or two and a second mode in which winds persists for 3 to 5 continuous days. This is clearly different from the degree of persistency observed under climatological conditions when winds persisted in one particular direction predominantly for few days. It was identified that during extreme events south-easterly winds dominated the first mode explaining 78% of the total occurrence in that mode and the westerly winds dominated the second mode explaining 86% of the total occurrence. In the latter case, when the winds persist for few days (3-5 days), the conditions are favourable for the long-range transport from the southern latitudes since circulation patterns (Fig. 5) are associated with typical frontal systems and baroclinic disturbances that make their way over Scandinavia.

4. Sensitivity of chosen events to cloud clearing procedure

As mentioned in Section 2, we allowed retrievals under cloudy conditions to be analysed, not only to have a robust number of samples, but also to avoid potential clear-sky biases. However, clouds can contaminate the NO_2 retrievals by modulating scattering in the atmosphere. Moreover, clouds are highly variable not only in space and time but also in their nature, thus making it challenging to assess their overall impact on the quality of retrievals. In the case of our study, potential cloud contamination can affect the selection of extreme events and thereby associated weather patterns that are being studied. Therefore, we carried out a sensitivity study wherein the entire analysis was repeated using only cloud screened NO_2 retrievals to investigate to what extent cloud clearing would affect the chosen events and subsequent analysis. We required that cloud fraction is less than 10% in AIRS data and valid retrievals of OMI cloud cleared tropospheric column NO_2 are available. Fig. 9 shows the histograms of NO_2 total columns under partially cloudy (solid lines) and cloud screened conditions (dotted lines). The histograms are accumulated over four seasons instead of months for clarity (to avoid too many lines). The chosen 90%ile thresholds are certainly different under partially cloudy and cloud screened conditions, but only slightly. We also found that, depending on the month, the selected extreme events match under partially cloudy and cloud screened conditions between 76% and 88% of the time. Fig. 10 further shows the spatial climatological distribution of NO_2 and during extreme events using only cloud screened retrievals. When compared to Fig. 3, the spatial distributions look patchy as a result of selected screening, but the magnitude and spatial features do not change significantly, providing confidence in our earlier analysis based on partially cloudy retrievals. Finally we evaluated if the events based on cloud screened data impact the analysis of meteorological conditions investigated here. Fig. 11 shows the vertical structure of specific humidity anomalies over the study region under partially cloudy (solid lines) and cloud screened conditions (dotted lines). While the slight differences in the vertical structure do exist, their sign and magnitudes are not large enough to change any previous argumentation.

5. Conclusions

The main aim of the present study was to characterize typical meteorological conditions associated with extreme NO_2 pollution events over Scandinavia. To that end, the study employs the bottom-up approach, in contrast to top-down approach taken by Thomas and Devasthale (2014) to study statistical co-variability of weather states and pollutant distribution. Such detailed analysis characterizing circulation patterns and meteorological conditions involving more than 300 extreme pollution events identified using satellite data has not been done before over the Scandinavian region. It is observed that the south-westerly winds dominated during extreme events accounting for 50-65% of total events, while the second largest annual occurrence was from south-easterly winds, accounting for 17% of total events followed by an equally similar contribution from north-westerly winds. Wind speeds are generally higher during extreme events, but only slightly, making it challenging to delineate distinct circulation regimes under these events. For the first time, we investigated the degree of persistency of wind direction during extreme events. In contrast to climatological conditions, two distinct modes of persistency were found; first one lasting a day or so and dominated by winds from south-easterly direction and the other mode lasting 3 to 5 days dominated by south-westerly and north-westerly winds. This information on the degree of persistency in conjunction with circulation patterns could be useful to identify extreme transport events. Further analysis of circulation patterns in combination with spatial distribution of humidity and its vertical structure suggest that these events occur as a result of long-range transport from southern latitudes, most likely from the northern parts of Germany and France, the Netherlands and Belgium. The analysis presented here provides information that can be used in the process oriented evaluation of chemistry transport models over Scandinavia.

Acknowledgements

We gratefully acknowledge OMI and AIRS Science Team and NASA GES DISC for providing data. The wind data from ERA-Interim reanalysis have been obtained from the ECMWF Data Server. MT acknowledges funding support from the Swedish Clean Air and climate research program of

IVL (Swedish Environmental Research Institute). Both MT and AD acknowledge Swedish National Space Board (grants 84/11:1, 84/11:2, Dnr: 94/16).

References

Beirle, S., Boersma, K. F., Platt, U., Lawrence, M. G., and Wagner, T.: Megacity Emissions and Lifetimes of Nitrogen Oxides Probed from Space, Science, 333, 1737–1739, doi:10.1126/science.1207824, 2011.

Bellander T, Wichmann J, and Lind T., Individual Exposure to NO2 in Relation to Spatial and Temporal Exposure Indices in Stockholm, Sweden: The INDEX Study. PLoS ONE 7(6): e39536. doi:10.1371/journal.pone.0039536, 2009.

Boersma, K. F., E. J. Bucsela, E. J. Brinksma, J. F. Gleason, NO2, OMI-EOS Algorithm Theoretical Basis Document: Trace Gas Algorithms: NO2, 4, 12-35, 2001. http://eospso.gsfc.nasa.gov/eos_homepage/for_scientists/atbd/docs/OMI/ATBD-OMI-04.pdf

Boersma, K. F., Jacob, D. J., Bucsela, E. J., Perring, A. E., Dirksen, R., van der A, R. J., Yantosca, R. M., Park, R. J., Wenig, M. O., and Bertram, T. H.: Validation of OMI tropospheric NO2 observations during INTEX-B and application to constrain NOx emissions over the eastern United States and Mexico, Atmos. Environ., 42, 4480–4497,doi:10.1016/j.atmosenv.2008.02.004, 2008.

Boersma, K. F., Eskes, H. J., Dirksen, R. J., van der A, R. J., Veefkind, J. P., Stammes, P., Huijnen, V., Kleipool, Q. L., Sneep, M., Claas, J., Leitão, J., Richter, A., Zhou, Y., and Brunner, D.: An improved tropospheric NO2 column retrieval algorithm for the Ozone Monitoring Instrument, Atmos. Meas. Tech., 4, 1905–1928, doi: 10.5194/amt-4-1905-2011, 2011.

Bucsela, E. J., Celarier, E. A., Wenig, M. O., Gleason, J. F., Veefkind, J. P., Boersma, K. F., and Brinksma, E. J.: Algorithm for NO2 vertical column retrieval from the ozone monitoring instrument, IEEE T. Geosci. Remote, 44, 1245–1258, doi:10.1109/TGRS.2005.863715, 2006.

Bucsela, E. J., Perring, A. E., Cohen, R. C., Boersma, K. F., Celarier, E. A., Gleason, J. F., Wenig, M. O., Bertram, T. H., Wooldridge, P. J., Dirksen, R., and Veefkind, J. P.: Comparison of tropospheric NO2 from in situ aircraft measurements with near-real-time and standard product data from OMI, J. Geophys. Res.,113, D16S31, doi:10.1029/2007JD008838, 2008.

Bucsela, E. J., Krotkov, N. A., Celarier, E. A., Lamsal, L. N., Swartz, W. H., Bhartia, P. K., Boersma, K. F., Veefkind, J. P., Gleason, J. F., and Pickering, K. E.: A new stratospheric and tropospheric NO_2 retrieval algorithm for nadir-viewing satellite instruments: applications to OMI, Atmos. Meas. Tech., 6, 2607-2626, doi:10.5194/amt-6-2607-2013, 2013.

Chahine, M. T and co-authors, AIRS: Improving Weather Forecasting and Providing New Data on Greenhouse Gases, Bull. Am. Meteorol. Soc., 87, 911–926, 2006.

Dee, D. P., Uppala, S. M., Simmons, A. J., Berrisford, P., Poli, P., Kobayashi, S., Andrae, U., Balmaseda, M. A., Balsamo, G., Bauer, P., Bechtold, P., Beljaars, A. C. M., van de Berg, L., Bidlot, J., Bormann, N., Delsol, C., Dragani, R., Fuentes, M., Geer, A. J., Haimberger, L., Healy, S. B., Hersbach, H., Hólm, E. V., Isaksen, L., Kållberg, P., Köhler, M., Matricardi, M., McNally, A. P., Monge-Sanz, B. M., Morcrette, J.-J., Park, B.-K., Peubey, C., de Rosnay, P., Tavolato, C., Thépaut, J.-N. and Vitart, F.: The ERA-Interim reanalysis: configuration and performance of the data assimilation system. Q.J.R. Meteorol. Soc., 137: 553–597, doi:10.1002/qj.828, 2011.

Devasthale, A. and M. A. Thomas, An investigation of statistical link between inversion strength and carbon monoxide over Scandinavia in winter using AIRS data, Atmospheric Environment, Vol. 56, 109-114 s, DOI: 10.1016/j.atmosenv.2012.03.042, 2012.

Devasthale et al. A decade of space borne observations of the Arctic atmosphere: novel insights from NASA's Atmospheric Infrared Sounder (AIRS) instrument. Bull. Amer. Meteor. Soc. doi:10.1175/BAMS-D-14-00202.1, in press, 2016.

Donnelly, A. A., Broderick, B. M. and Misstear, B. D.: The effect of long-range air mass transport pathways on PM10 and NO2 concentrations at urban and rural background sites in Ireland: Quantification using clustering techniques, J Environ Sci Health A Tox Hazard Subst Environ Eng., doi: 10.1080/10934529.2015.1011955, 2015.

Eckhardt, S., A. Stohl, S. Beierle, N. Spichtinger, P. James, C. Forster, C. Junker, T. Wagner, U. Platt, and S. G. Jennings, 2003: The North Atlantic Oscillation controls air pollution transport to the Arctic, Atmos. Chem. Phys., 3, 1769-1778, 2003.

Ehhalt, D. H., Rohrer, F., and Wahner, A.: Sources and Distribution of NO x in the Upper Troposphere at Northern Mid-Latitudes, J. Geophys. Res., 97, 3725–3738, http://www.agu.org/journals/jd/v097/iD04/91JD03081/, 1992.

Geddes JA, et al. Long-term trends worldwide in ambient NO_2 concentrations inferred from satellite observations. Environ Health Perspect 1243281–289.2892016, doi:10.1289/ehp.1409567, 2016.

Gustafsson, M., H. Orru, B. Forsberg, S. Åström, H. Tekie, K. Sjöberg, Quantification of population exposure to NO2, PM2.5 and PM10 in Sweden 2010, Swedish Environmental Research Institute (IVL), IVL Report B2197, pp. 74, December 2014.

Klingberg, J., M. P. Björkman, G. P. Karlsson, and H. Pleijel, Observations of Ground-level Ozone and NO2 in Northernmost Sweden, Including the Scandian Mountain Range, AMBIO, 38(8):448-451. doi: http://dx.doi.org/10.1579/0044-7447-38.8.448, 2009.

Lamarque, J.-F. and Dentener, F. and McConnell, J. and Ro, C.-U. and Shaw, M. and Vet, R. and Bergmann, D. and Cameron-Smith, P. and Dalsoren, S. and Doherty, R. and Faluvegi, G. and Ghan, S. J. and Josse, B. and Lee, Y. H. and MacKenzie, I. A. and Plummer, D. and Shindell, D. T. and Skeie, R. B. and Stevenson, D. S. and Strode, S. and Zeng, G. and Curran, M. and Dahl-Jensen, D. and Das, S. and Fritzsche, D. and Nolan, M., Multi-model mean nitrogen and sulfur deposition from the Atmospheric Chemistry and Climate Model Intercomparison Project (ACCMIP): evaluation of historical and projected future changes, Atmos. Chem. Phys., 13, 7997-8018,2013.

Lamsal LN, Martin RV, van Donkelaar A, Celarier EA, Bucsela EJ, Boersma KF, et al. Indirect validation of tropospheric nitrogen dioxide retrieved from the OMI satellite instrument: insight into the seasonal variation of nitrogen oxides at northern midlatitudes. J Geophys Res 115D05302; doi:10.1029/2009JD013351 , 2010.

Lamsal LN, Martin RV, van Donkelaar A, Steinbacher M, Celarier EA, Bucsela E, et al. Ground-level nitrogen dioxide concentrations inferred from the satellite-borne Ozone Monitoring Instrument. J Geophys Res 113D16308; .10.1029/2007JD009235, 2008.

Lamsal, L. N., Krotkov, N. A., Celarier, E. A., Swartz, W. H., Pickering, K. E., Bucsela, E. J., Gleason, J. F., Martin, R. V., Philip, S., Irie, H., Cede, A., Herman, J., Weinheimer, A., Szykman, J. J., and Knepp, T. N.: Evaluation of OMI operational standard NO_2 column retrievals using in situ and surface-based NO_2 observations, Atmos. Chem. Phys., 14, 11587-11609, doi:10.5194/acp-14-

11587-2014, 2014.

Miyazaki, K. and Eskes, H. and Sudo, K. and Boersma, K. F. and Bowman, K. and Kanaya, Y., Decadal changes in global surface NOx emissions from multi-constituent satellite data assimilation, Atmos. Chem. Phys., 17, 2017, 807-837, doi:10.5194/acp-17-807-2017.

Nilsson Sommar, J., A. Ek, R. Middelveld, A. Bjerg, S-E. Dahlén, C. Janson, B. Forsberg, Quality of life in relation to the traffic pollution indicators NO2 and NOx: results from the Swedish GA2LEN survey, BMJ Open Resp Res 2014;1:1 e000039 doi:10.1136/bmjresp-2014-000039.

Oudin, A., L. Bråbäck, D. Oudin Åström, M. Strömgren, and B. Forsberg, Association between neighbourhood air pollution concentrations and dispensed medication for psychiatric disorders in a large longitudinal cohort of Swedish children and adolescents, BMJ Open 2016;6:6 e010004 doi:10.1136/bmjopen-2015-010004, 2016.

Richter A, Burrows JP, Nüss H, Granier C, Niemeier U. Increase in tropospheric nitrogen dioxide over China observed from space. Nature 437129–132.132; doi:10.1038/nature04092, 2005.

Schneider, P., Lahoz, W. A., and van der A, R.: Recent satellite-based trends of tropospheric nitrogen dioxide over large urban agglomerations worldwide, Atmos. Chem. Phys., 15, 1205-1220, doi:10.5194/acp-15-1205-2015, 2015.

Sjöberg K., M. Haeger-Eugensson, M. Lijeberg, H. Blomgren, and B. Forsberg, Quantification of population exposure to nitrogen dioxide in Sweden, Swedish Environmental Research Institute (IVL), IVL Report B1579, pp. 31, September 2004.

Stohl, A., Huntrieser, H., Richter, A., Beirle, S., Cooper, O. R., Eckhardt, S., Forster, C., James, P., Spichtinger, N., and Wenig, M.: Rapid intercontinental air pollution transport associated with a meteorological bomb, Atmos. Chem. Phys., 3, 969–985, 2003, http://www.atmos-chem-phys.net/3/969/2003/.

Schaub, D., Weiss, A. K., Kaiser, J. W., Petritoli, A., Richter, A., Buchmann, B., and Burrows, J. P.: A transboundary transport episode of nitrogen dioxide as observed from GOME and its impact in the Alpine region, Atmos. Chem. Phys., 5, 23–37, doi:10.5194/acp-5-23-2005, 2005.

Susskind, J., J. M. Blaisdell and L. Iredell, Improved methodology for surface and atmospheric soundings, error estimates and quality control procedures: the atmospheric infrared sounder science team version-6 retrieval algorithm, J. Appl. Remote Sens., 8(1), 084994, doi:10.1117/1.JRS.8.084994, 2014.

Taj T, Stroh E, Åström DO, Jakobsson K, Oudin A., Short-Term Fluctuations in Air Pollution and Asthma in Scania, Sweden. Is the Association Modified by Long-Term Concentrations? PLoS ONE 11(11): e0166614. doi:10.1371/journal.pone.0166614, 2016.

Thomas, M. A. and Devasthale, A.: Sensitivity of free tropospheric carbon monoxide to atmospheric weather states and their persistency: an observational assessment over the Nordic countries, Atmos. Chem. Phys., 14, 11545-11555, doi:10.5194/acp-14-11545-2014, 2014.

van der A, R. J., H. J. Eskes, K. F. Boersma, T. P. C. van Noije, M. Van Roozendael, I. De Smedt, D. H. M. U. Peters, and E. W. Meijer, Trends, seasonal variability and dominant NOx source derived from a ten year record of NO2 measured from space, J. Geophys. Res., 113, D04302, doi:10.1029/2007JD009021, 2008.

Vasilkov, A. P., Joiner, J., Oreopoulos, L., Gleason, J. F., Veefkind, P., Bucsela, E., Celarier, E. A., Spurr, R. J. D., and Platnick, S.: Impact of tropospheric nitrogen dioxide on the regional radiation budget, Atmos. Chem. Phys., 9, 6389-6400, doi:10.5194/acp-9-6389-2009, 2009.

Wenig, M., Spichtinger, N., Stohl, A., Held, G., Beirle, S., Wagner, T., Jähne, B., and Platt, U.: Intercontinental transport of nitrogen oxide pollution plumes, Atmos. Chem. Phys., 3, 387–393, doi:10.5194/acp-3-387-2003, 2003.

Zhang, Q., et al., NOx emission trends for China, 1995–2004: The view from the ground and the view from space, J. Geophys. Res., 112, D22306, doi:10.1029/2007JD008684, 2007.

Zien, A. W., Richter, A., Hilboll, A., Blechschmidt, A.-M., and Burrows, J. P.: Systematic analysis of tropospheric NO2 long-range transport events detected in GOME-2 satellite data, Atmos. Chem. Phys., 14, 7367–7396, doi: 10.5194/acp-14-7367-2014, 2014.

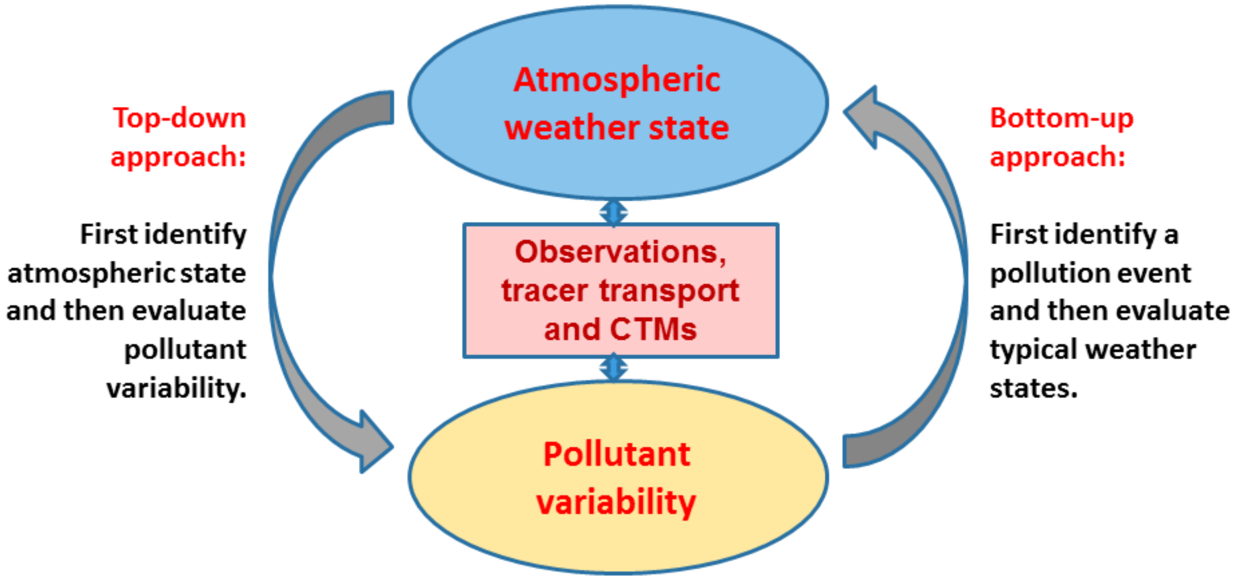

Fig. 1: Schematic showing two different approaches to study statistical co-variability of atmospheric weather states and pollutant concentrations.

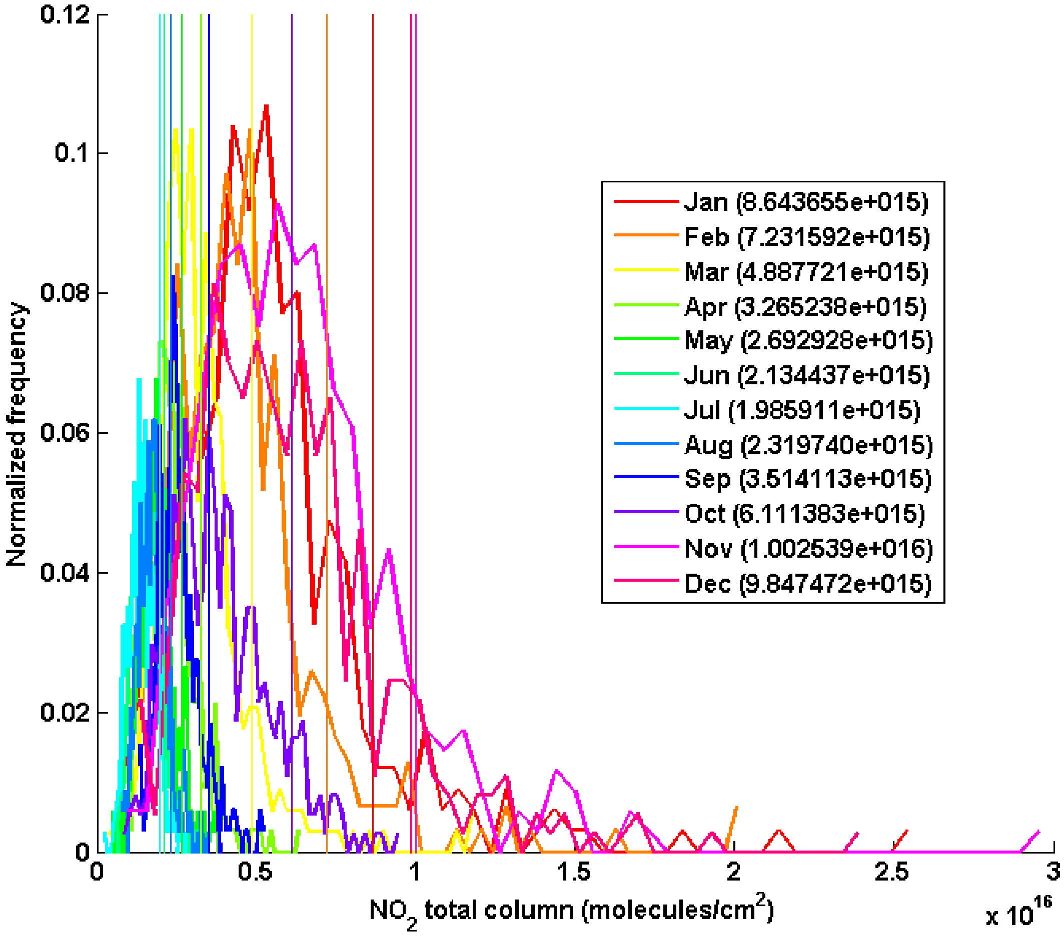

Fig. 2: Monthly histograms of tropospheric total column NO_2 over the centre of the study area (55N-60N, 11E-20E) and corresponding 90%ile thresholds (shown by vertical lines and values in brackets).

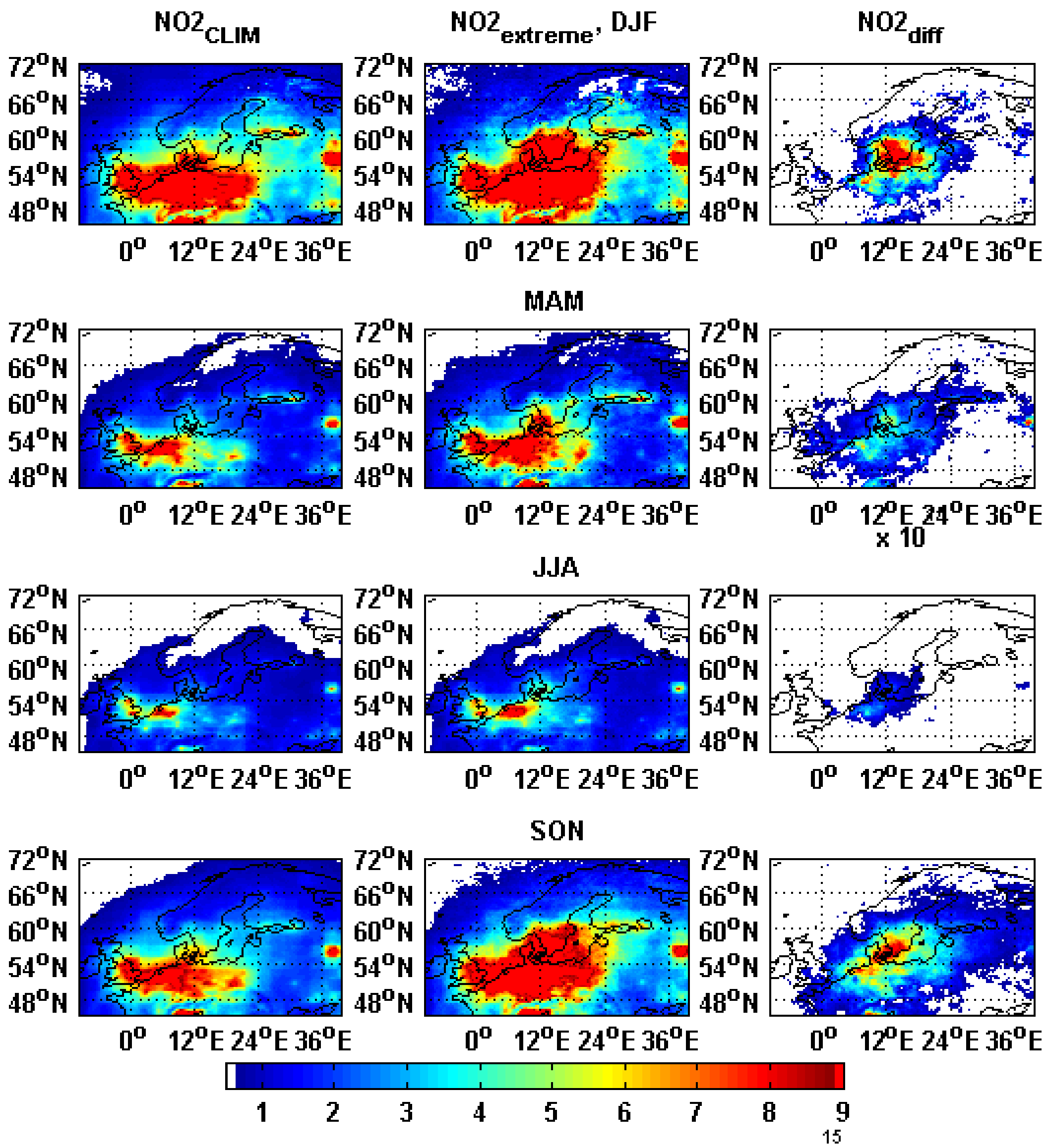

Fig, 3: Seasonal, climatological average tropospheric NO_2 total column (first column) based on nearly 11-yr OMI data (2004-2015), NO_2 distribution during extreme events (second column) and the difference between the two (third column). The units are in molecules/cm^2.

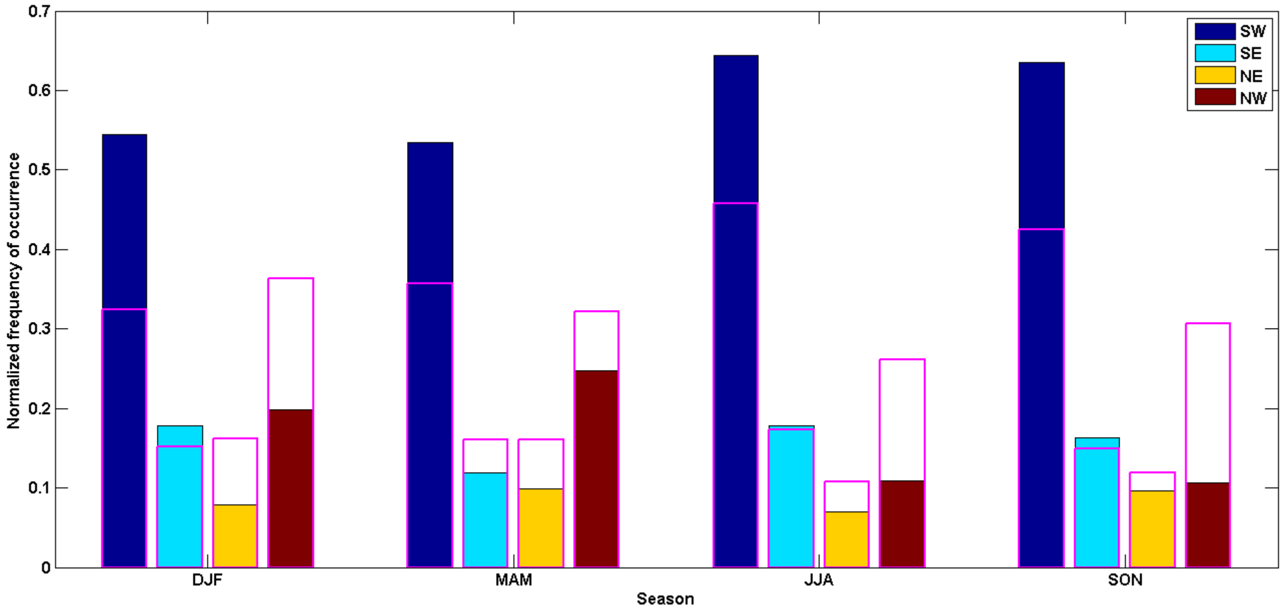

Fig. 4: Seasonal normalized frequency of occurrence of a particular wind direction at 850 hPa when NO_2 extreme pollution events were observed. The hollow magenta bars show normalized frequency under climatological conditions.

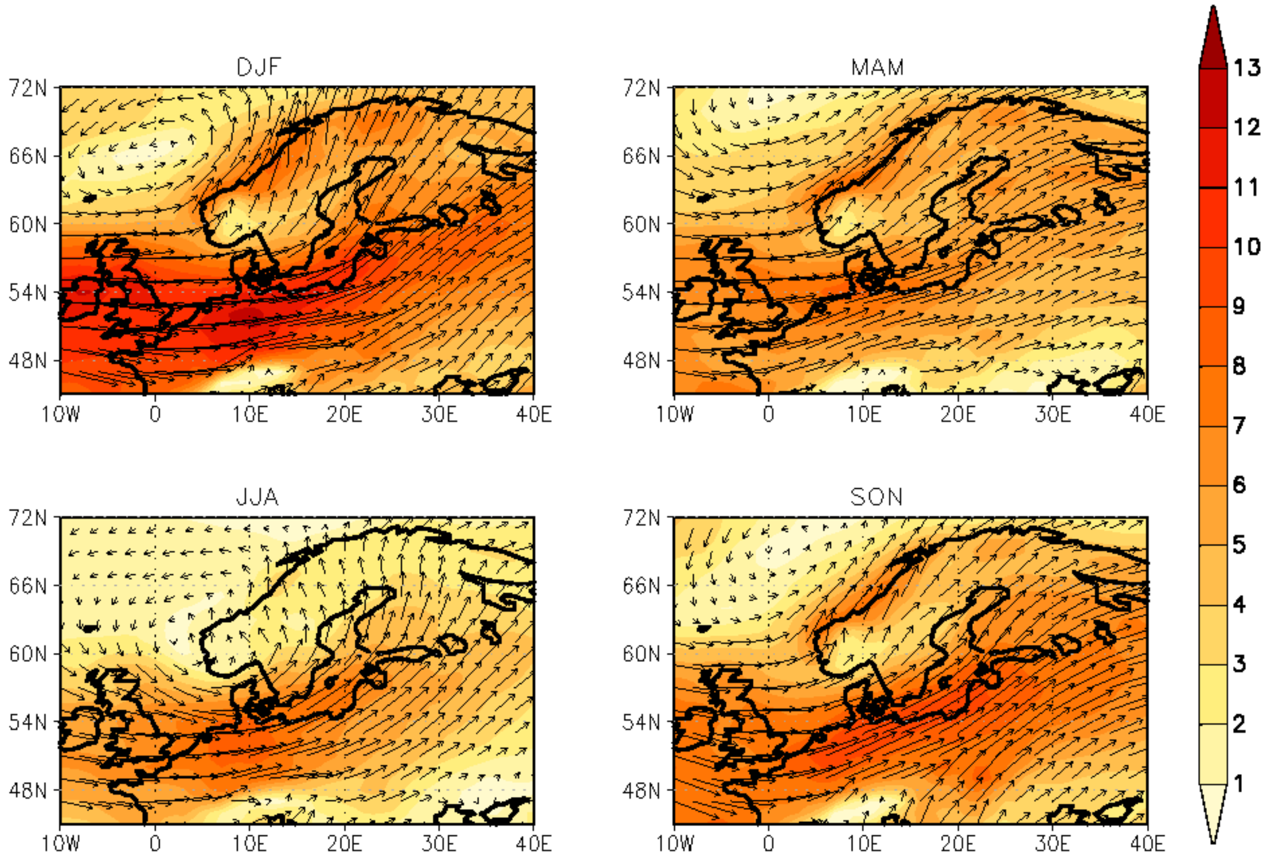

Fig. 5: Seasonal average wind strengths and direction at 850 hPa showing dominant circulation pattern observed when NO_2 extreme pollution events occur.

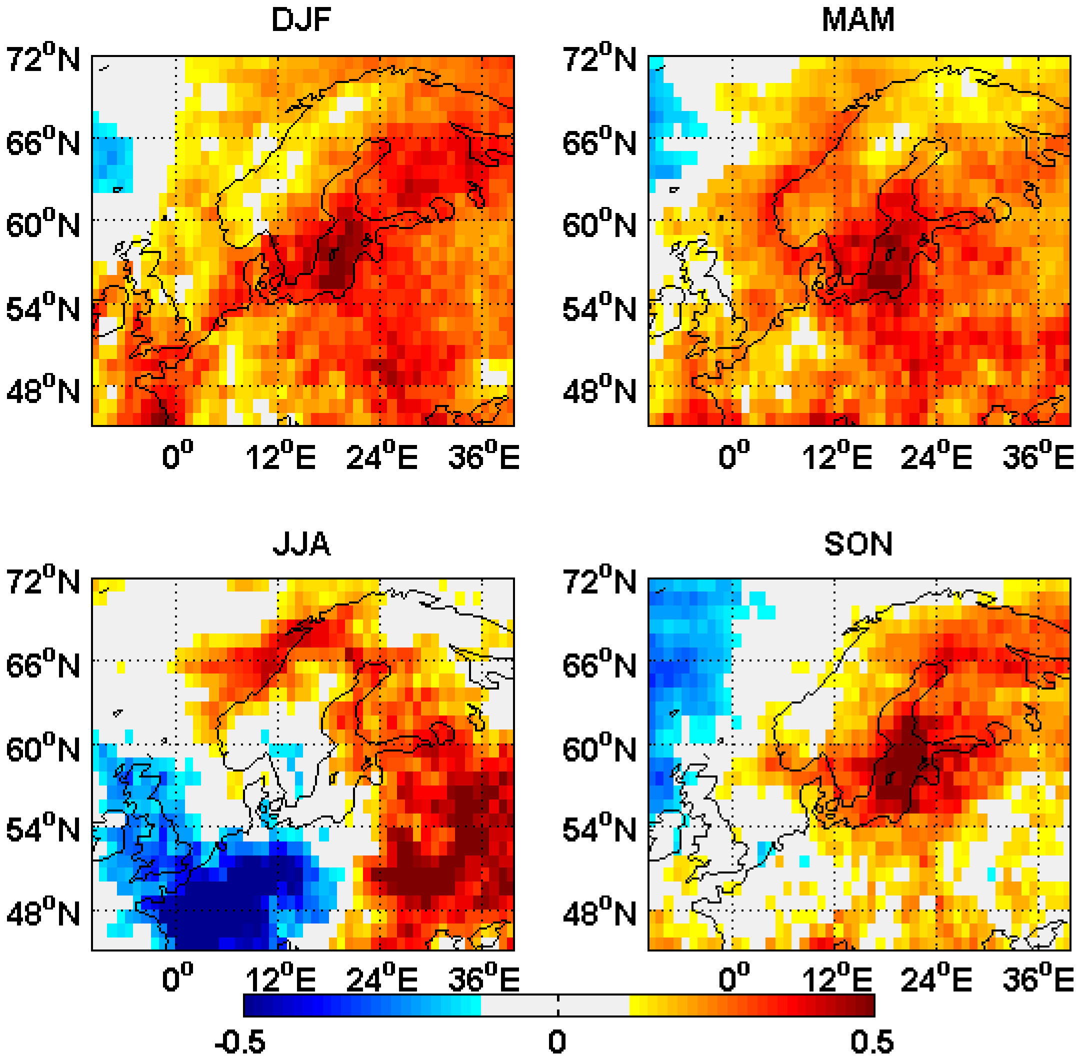

Fig. 6: The seasonal spatial patterns of specific humidity anomalies (g/kg) during extreme NO_2 pollution events.

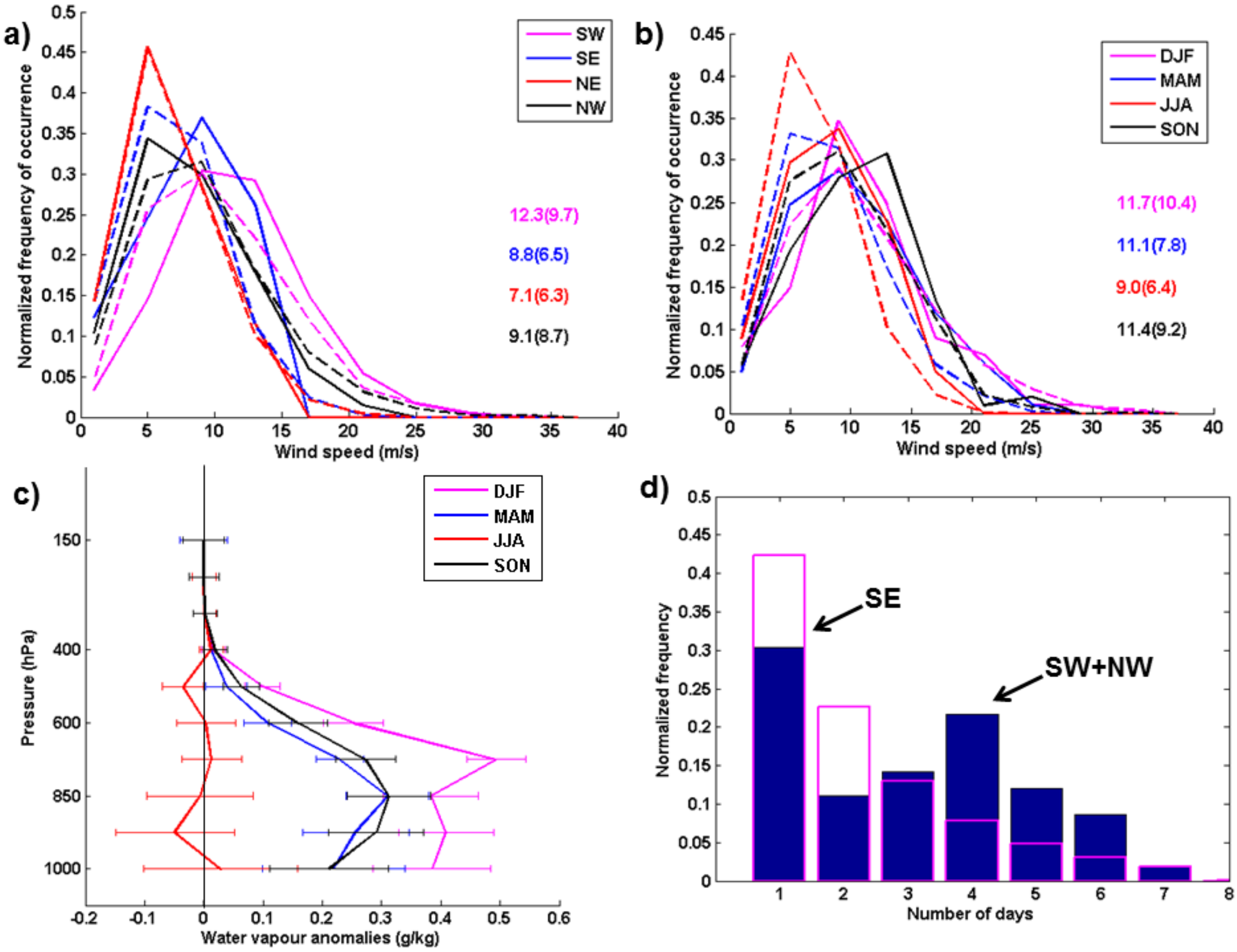

Fig. 7: a) Histograms of wind speeds (m/s) at 850 hPa over the center of the study area (55N-60N, 11E-20E) during extreme events (solid lines) and climatological conditions (dotted lines, 2004-2015) when data are partitioned for different wind directions. The numbers show average wind speeds (m/s) during extreme events and in brackets under climatological conditions. b) Same as in (a), but when wind data are partitioned for different seasons. c) Vertical anomalies of specific humidity (g/kg) during extreme events with horizontal bars showing standard deviations. d) Persistency of wind directions as a function of number of continuous days. The magenta bars show persistency under climatological conditions.

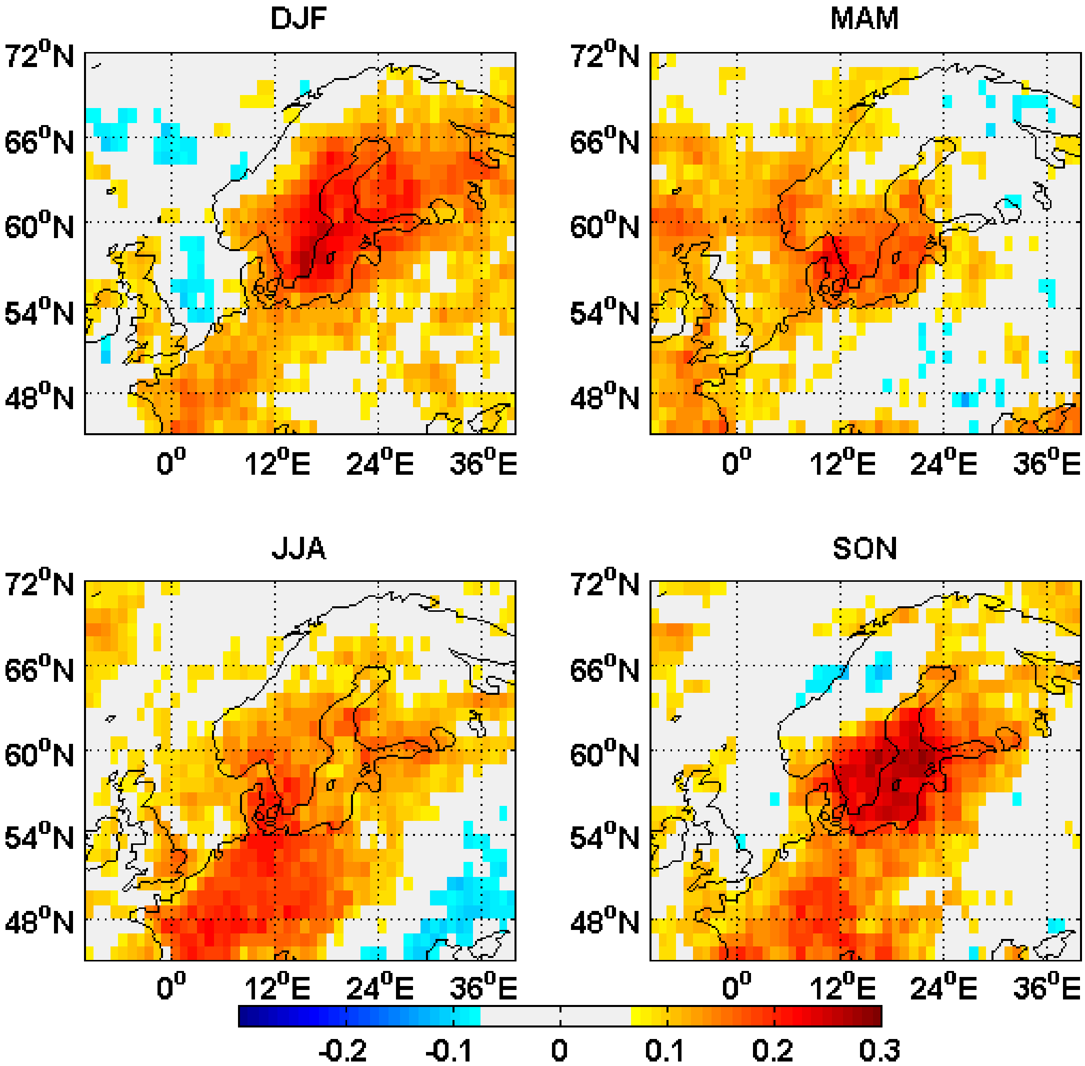

Fig. 8: Total cloud fraction anomalies observed during extreme events based on AIRS data.

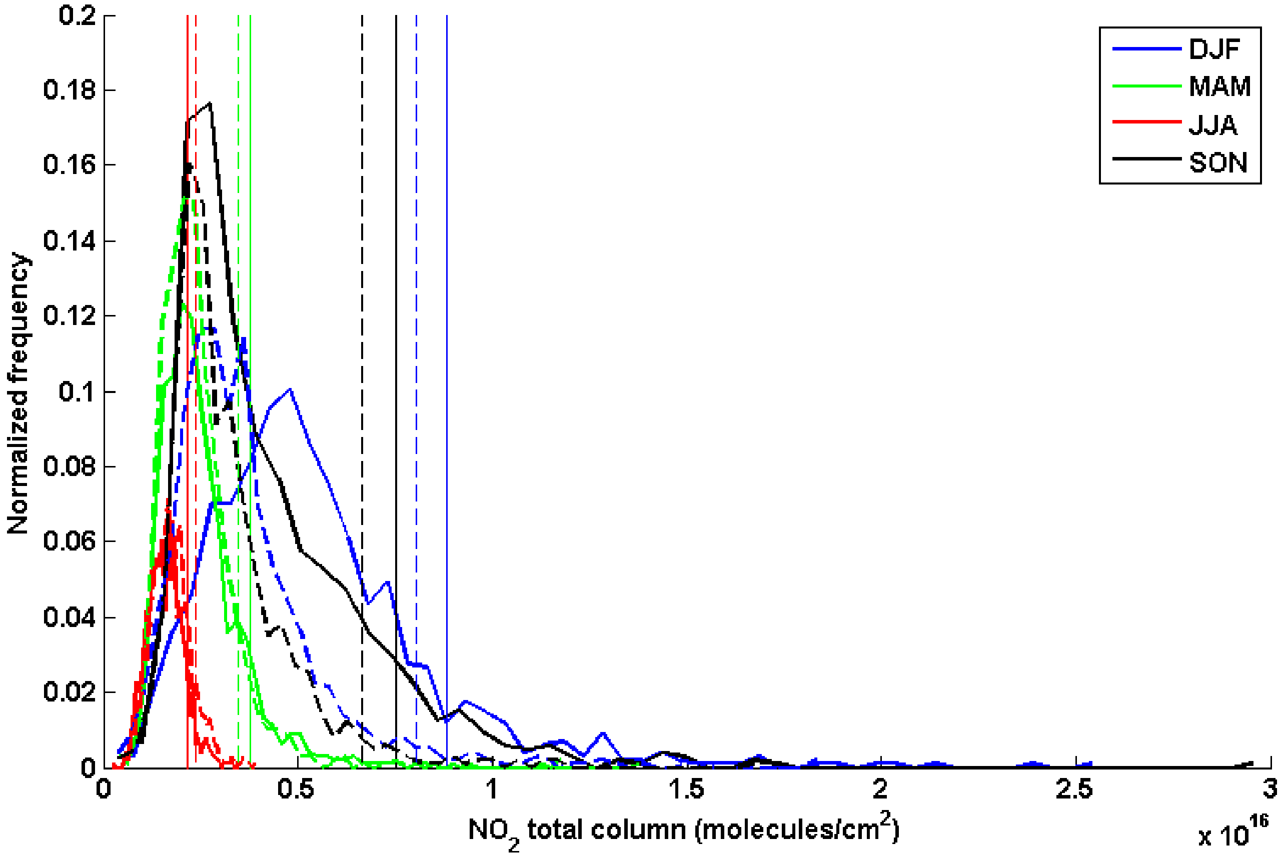

Fig. 9: Seasonal histograms of total column tropospheric NO_2 over the centre of the study area (55N-60N, 11E-20E) and corresponding 90%ile thresholds (shown by vertical lines). The solid lines show histograms based on retrievals under partially cloudy conditions, while the dotted lines show histograms based only on cloud cleared retrievals.

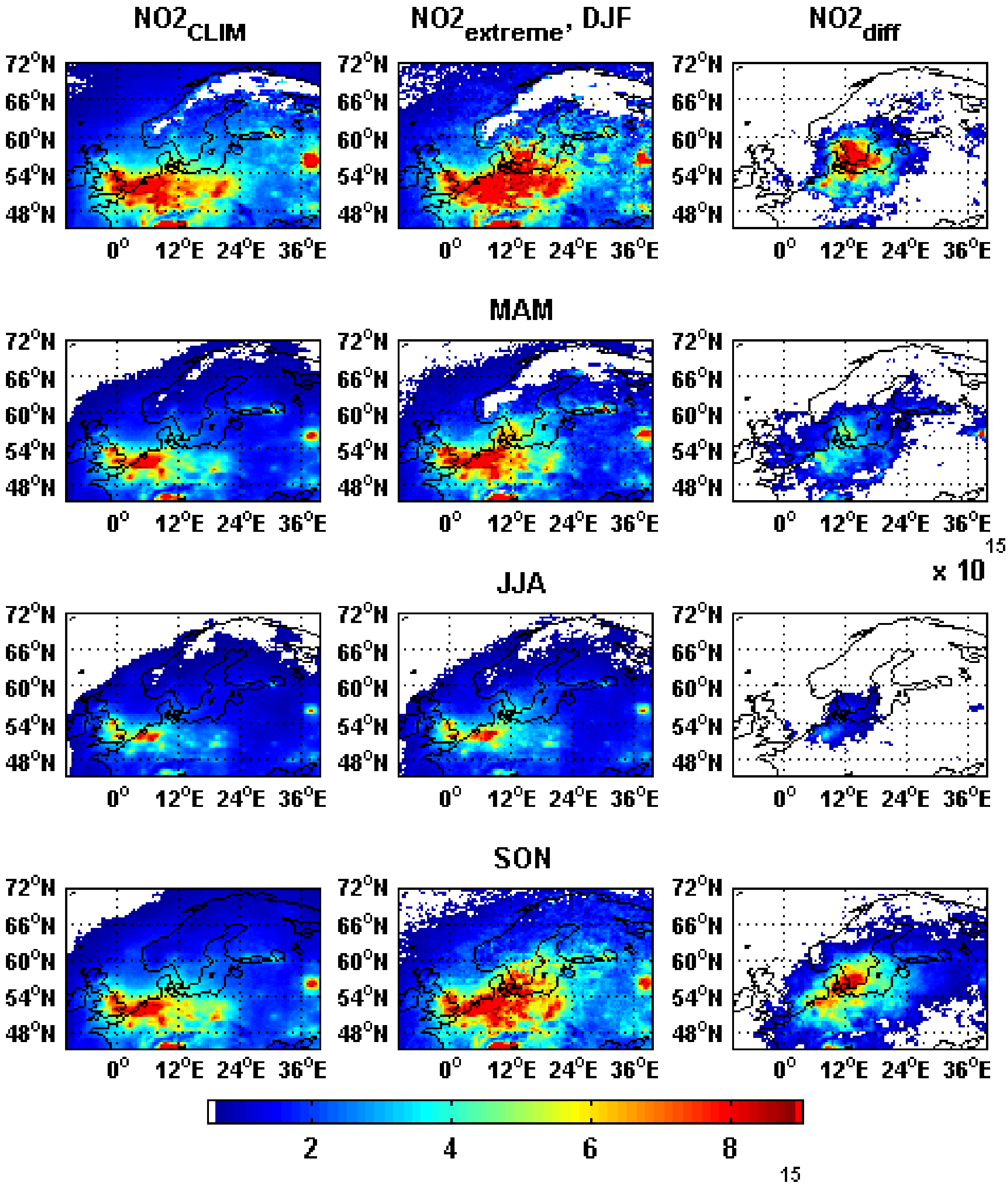

Fig. 10: Seasonal, climatological average tropospheric NO_2 total column (first column) based only on cloud screened OMI data (2004-2015), NO_2 distribution during extreme events (second column, also based on cloud screened data) and the difference between the two (third column). The units are in molecules/cm^2.

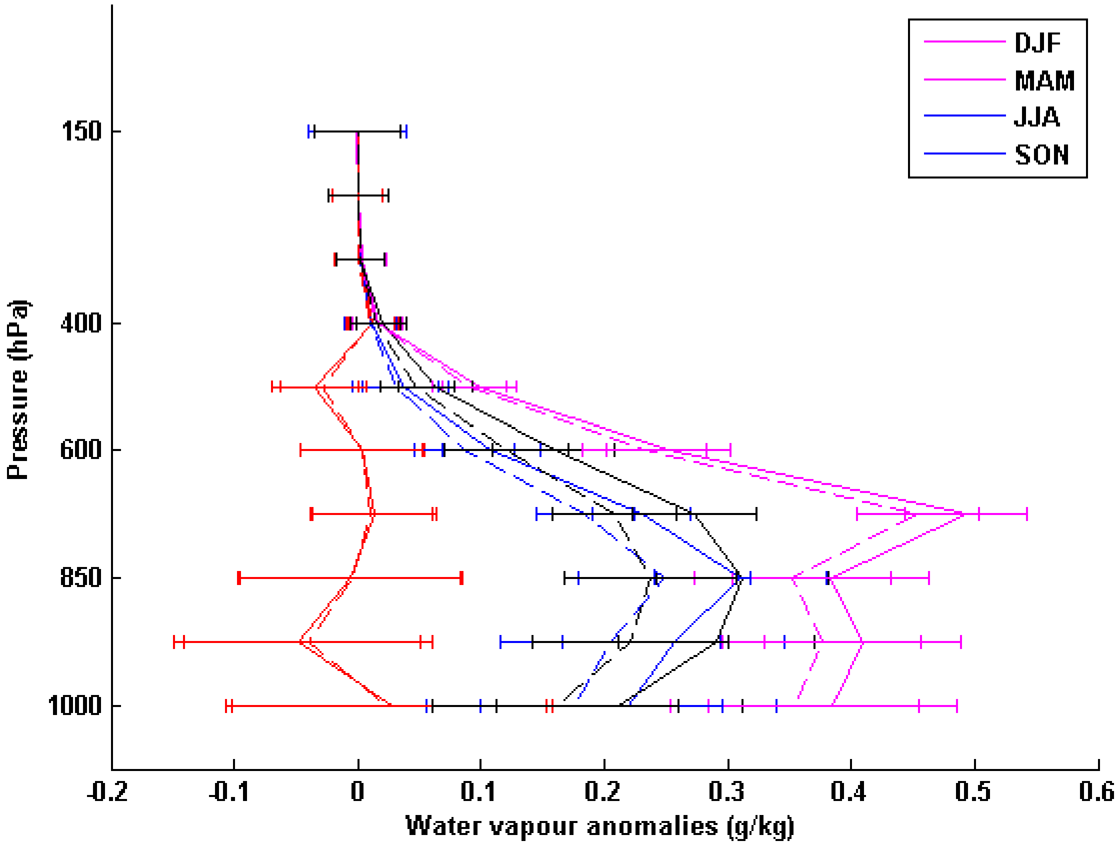

Fig. 11: Vertical anomalies of specific humidity (g/kg) during extreme events with horizontal bars showing standard deviations. The solid lines show anomalies under partially cloudy retrievals and dotted lines based on cloud screened retrievals.